Active Fault Management for Microgrids

Wenfeng Wan, Yan Li, Bing Yan, Mikhail Bragin, Jason Philhower, Peng Zhang, Peter Luh
Department of Electrical and Computer Engineering
University of Connecticut
Storrs, CT 06269, USA

Guy Warner
Pareto Energy
Washington, DC 20037, USA

***Abstract*—Fault management is critical for efficiently supporting the increasing microgrids' penetration in distribution networks but remains an open problem. No existing ride through methods can ride through symmetrical and asymmetrical faults without increasing the fault current magnitude, meanwhile balancing microgrid power and eliminating double frequency ripples in microgrid inverters. The paper bridges this gap by contributing a novel active fault management (AFM) method. The new contributions include: 1) the development of a new conceptual AFM to control multiple variables during voltage dips; 2) the optimization-based AFM to coordinate different objectives according to a guidance and 3) a combined optimization and feedback control, during which optimization method provides the optimal trade-offs among different objectives and the feedback control ensures accurate realization of chosen operation points. Simulations with different types of faults prove that the developed AFM can achieve better trade-offs and coordination among various control objectives in comparison to the conventional ride through method.**

Keywords—active fault management, microgrids, faults, optimization, Pareto frontier

I. INTRODUCTION

Fault management for microgrids is essential to keep microgrids' normal operation and to support the main grid's stability and recovery [1]. The IEEE and North American Electric Reliability Corporation have recently proposed their specific requirements on distributed energy resources and microgrids during voltage sags [2, 3]. One critical new requirement is the low voltage ride through, which means microgrids are required to stay connected with the main grid for a specified period during voltage sags.

Riding through a fault, however, creates significant challenges for both microgrids and the main grid. First, microgrids that stay connected during faults can unfavorably contribute excessive fault currents to the main grid. The fault current contributions may soon exceed the designed capacities of the grid components (e.g. transformers, circuit breaker, and surge arresters) when many microgrids are consecutively tied into the grid facilities, which would lead to costly upgrades. Also, the sudden change in power delivery owing to voltage changes and occurrence of double-line-frequency power ripples harm microgrids' converters [4].

This material is based upon work supported by the National Science Foundation under Grant Nos. 1611095 and 1647209, and by funding from the Office of the Provost, University of Connecticut.

One way to limit microgrids' contribution to fault currents is to install extra hardware, such as current limiters [5] and dynamic voltage restorers [6]. Recovery time for some of those devices is long and thus is not favorable for the main grid's recovery. Also, electrical loss and installation cost of microgrids would be increased. Researchers have also designed various advanced control strategies for microgrids' interface converters, which are used to connect the main grid and other parts of microgrids. In [7], the magnitude of fault currents is controlled by changing phase angles of converters' currents during balanced faults only without considering unbalanced faults and other important variables, e.g., power transfer between microgrids and the main grid. During unbalanced faults, double-line-frequency power ripples have been eliminated for renewable generation [8]. However, fault current contributions have not been considered.

Existing fault managements for microgrids mostly focus on controlling one variable, such as fault currents, while other critical variables, such as power balance and power ripples, are not controlled. However, all the important variables, e.g., power balance, current limits, power ripples and fault currents, affect the main grid and microgrids' operation and stability during faults [4]. Challenges arise when multiple variables are considered simultaneously. Firstly, satisfying multiple objectives would result in either the increase of capacitor's voltage or the increase of inverter's output current beyond safety thresholds. Better performance of one objective worsens the performance of other objectives. A guidance should be designed to find the optimal trade-offs among multiple objectives to optimize a microgrid's performance. Lastly, after the trade-offs are chosen, the controller design should be based on those trade-offs and selected operation points.

In this paper, an active fault management (AFM) scheme has been developed to manage microgrids during balanced and unbalanced faults. The AFM is extensive. It takes into consideration various variables and concerns, such as safety thresholds, power balance, fault currents and power ripples, rather than one concern. The AFM is optimization-based. Pareto frontiers, functioning as selection guidance, are leveraged to identify the best trade-offs among various objectives. Also, AFM is integrative of optimization and feedback control. Optimization is to provide guidance for operation points while the operation-point-dependent feedback control is to ensure accuracy. Simulation results for different types of faults demonstrate that AFM is capable of coordinately managing multiple objectives and constraints.

978-1-5090-6683-4/18/$31.00 ©2018 IEEE

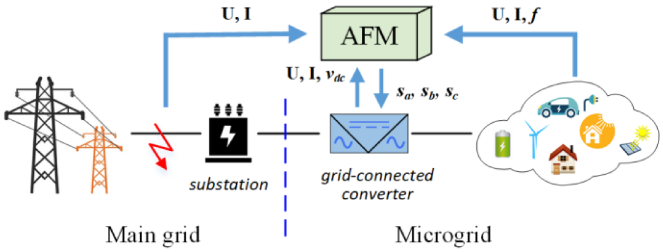

Fig. 1. Schematic of AFM for microgrids.

II. Active Fault Management Scheme

This section first describes AFM's objectives and constraints. Then, AFM is formulated as an optimization problem, which is solved by fmincon interior-point algorithm in Matlab/Simulink.

A. Management objectives

IEEE Std 1547 has mandated three capabilities during fault for microgrids: 1. keep connected with the main power grid for a voltage-sag dependent period; 2. keep synchronism with the main grid; 3. restore output as required after fault [2]. The converters' available capacity, high controllability and fast response enable the management of multiple objectives. Although very few North American utility companies have yet approved microgrid-to-utility grid interconnection through converters, such an interconnection has been more commonly approved outside of North America [9, 10].

Two constraints in AFM include power balance and current safety limits. Power balance ensures that active power output before faults equal to active power after faults. During faults, without increasing the microgrid's currents, its output power decreases. Such an abrupt decrease in power delivery can result in overvoltage in DC links. Also, the amplitude of currents should be less than 2 pu to prevent overcurrent damages.

The first management objective in AFM is to ensure that microgrids do not contribute to increasing fault currents' amplitudes. With this objective being met, the previously installed devices in the distribution system won't be damaged. If fault currents increase after microgrids' connection, the original devices have to be replaced by those with higher ratings. This is costly when a large number of devices should be replaced.

The second management objective is to eliminate double-line-frequency ripples in microgrids' active power. During symmetrical conditions, the output power from microgrids to distribution system is a constant value. During asymmetrical faults, microgrids' active power would contain double-line-frequency components. These components would harm microgrids' inverters and also can compromise power quality and even trip certain devices due to non-sinusoidal current and voltage references.

B. Problem Formation

The active fault management for microgrids during fault is formulated as a optimization problem. There are two components in the objective function. One is microgrids' fault current contributions, i.e., the difference between fault currents from the main grid and the total fault current to the ground. The second component is the magnitude of double-line frequency ripples in microgrids' active power. Constraint (3) is power balance. Constraints (4) are to guarantee that the sum of inverter's three-phase currents is zero. Constraints (5) are current safety limits. Equations are given with per-unit systems and rectangular coordinates.

$$\text{minimize } mO_1 + (1-m)O_2, \quad m \in [0,1] \tag{1}$$

$$\begin{cases} O_1 \equiv \sum_k |d_k| \\ O_2 \equiv \frac{1}{3}\frac{\sqrt{\left[\sum_i (U_{ix}I_{ix} - U_{iy}I_{iy})\right]^2 + \left[\sum_i (U_{iy}I_{ix} + U_{ix}I_{iy})\right]^2}}{P_1} \\ d_k \equiv \frac{\sqrt{(k_{T1}I_{kx} + k_{T2}I_{ky} + I_{kMx})^2 + (k_{T3}I_{kx} + k_{T4}I_{ky} + I_{kMy})^2}}{\sqrt{I_{kMx}^2 + I_{kMy}^2}} - 1 \end{cases}$$

$$(i = a, b, c;\ k = a, b, c) \tag{2}$$

subject to

$$\tfrac{1}{3}(U_{ax}I_{ax} + U_{ay}I_{ay} + U_{bx}I_{bx} + U_{by}I_{by} + U_{cx}I_{cx} + U_{cy}I_{cy}) = P_1 \tag{3}$$

$$\begin{cases} I_{ax} + I_{bx} + I_{cx} = 0 \\ I_{ay} + I_{by} + I_{cy} = 0 \end{cases} \tag{4}$$

$$\begin{cases} \sqrt{I_{ax}^2 + I_{ay}^2} \le 2\ pu \\ \sqrt{I_{bx}^2 + I_{by}^2} \le 2\ pu \\ \sqrt{I_{cx}^2 + I_{cy}^2} \le 2\ pu \end{cases} \tag{5}$$

where m is the weight factor. Phases i are phase a, b and c. Phases k are the fault phases. k_{T1}, k_{T2}, k_{T3}, k_{T4} are introduced to represent the effect of transformer on converters' currents, e.g., amplitude changes and angle shifts. I_{kMx} and I_{kMy} are the real part and imaginary part, respectively, of fault currents from the main grid at fault location. P_1 is microgrids' output active power before fault.

In rectangular coordinates, the converter's three-phase voltages and currents are expressed as,

$$\begin{cases} \mathbf{U_A} = U_{ax} + jU_{ay} \\ \mathbf{U_B} = U_{bx} + jU_{by} \\ \mathbf{U_C} = U_{cx} + jU_{cy} \end{cases} \tag{6}$$

$$\begin{cases} \mathbf{I_A} = I_{ax} + jI_{ay} \\ \mathbf{I_B} = I_{bx} + jI_{by} \\ \mathbf{I_C} = I_{cx} + jI_{cy} \end{cases} \tag{7}$$

Fig. 1 shows the schematic of AFM for microgrids. After faults are detected, the management system starts to operate. The optimization module calculates converters' reference currents based on (1)-(7). The feedback control module is added to ensure control accuracy. Without feedback control, the control accuracy would be compromised owing to measurement and calculation errors.

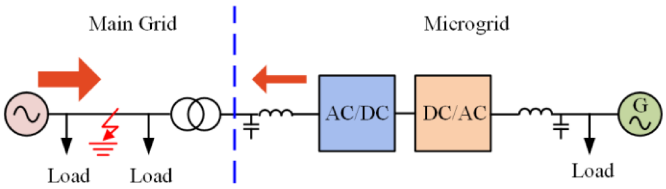

Fig. 2. Schematic of the studied system.

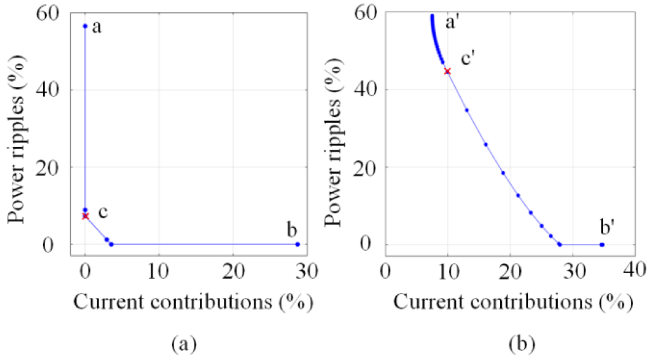

Fig. 3. Pareto frontiers for (a) single-phase-to-ground fault and (b) double-phase-to-ground fault.

III. Case Study

This section justifies the developed AFM with Matlab/Simulink simulations. Resistive faults are simulated. The simulation results are achieved with voltages sags of 0.3 pu. A conventional ride through method is used for comparison and it has only one objective: keeping power balance under the constraint of current safety limits.

A. System Description

The schematic of the studied system is shown in fig. 2. During normal condition, the microgrid has a total generation of 4.21 MW, and no reactive power is generated or absorbed. The total load within the microgrid is 3.30 MW. The left 0.91 MW is delivered to the grid through a grid-connected converter (GCC) [9]. The rated phase-to-phase voltage of the microgrid is 2.90 kV. In our study, faults happen at the main grid. During simulation, the GCC's output voltages, currents, and its capacitor's voltages are measured. The instantaneous active power injected by GCC to point of common connection (PCC) is also measured. At the fault location, fault currents from the main grid, fault currents from the microgrid and the total fault currents to the ground are measured.

B. Pareto Frontier

As shown in the objective function (1), before simulation, the weight factor m needs to be selected first. The Pareto frontier, acting as selection guidance, is the best possible trade-offs between the fault current contribution objective O_1 and the power ripple objective O_2 [11], and thus is used as a selection guidance. The Pareto frontiers for single-phase-to-ground fault and double-phase-to-ground fault are shown in Fig. 3. There is no Pareto frontier for three-phase-to-ground fault, because O_2 is inherently zero owing to symmetry, and only O_1 is left in the objective function.

The Pareto frontiers are achieved by giving m in (1) different values from 0 to 1 with a step size of 0.02. The points marked with a and a' are obtained with $m = 1$, namely minimizing fault current contributions without considering double-line frequency power ripples. The points marked with b and b' are obtained with $m = 0$, namely minimizing power ripples without considering fault current contributions.

Operators can choose operation points on the Pareto frontiers according to their requirements and priority on power ripples and fault current contributions. In our following simulations,

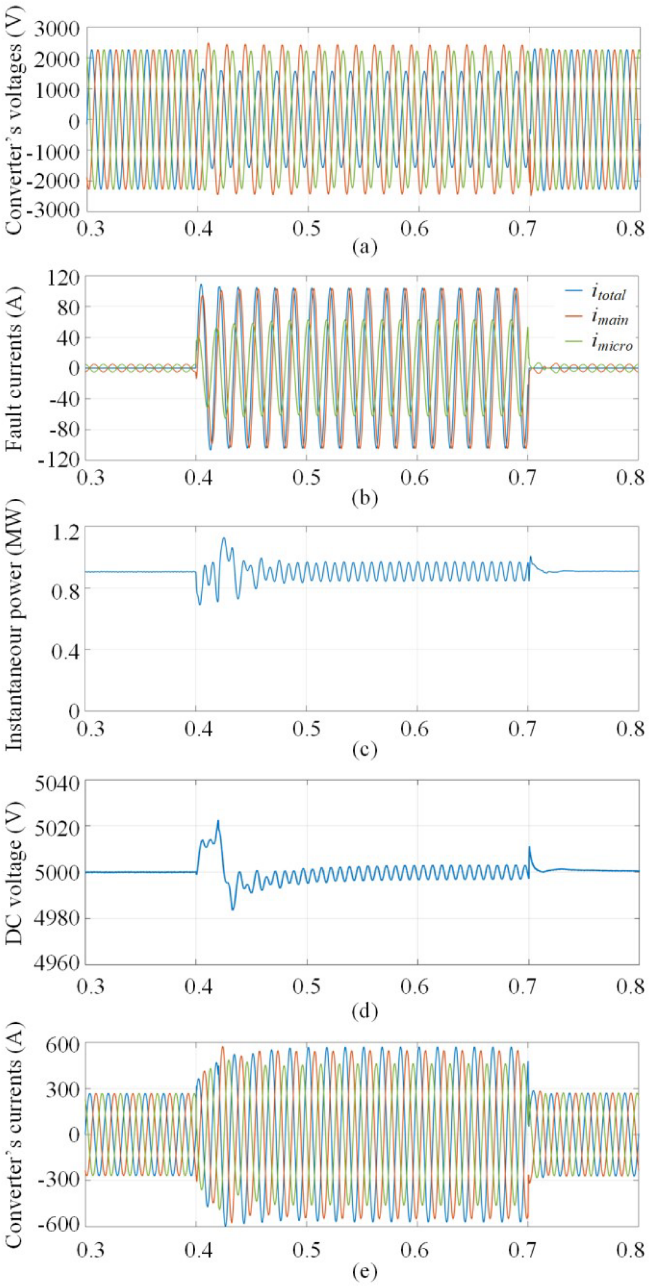

Fig. 4 Simulation results for single-phase-to-ground faults with AFM. (a) the converter's output voltages; (b) fault currents at fault location. i_{total} is the total fault currents to the ground, i_{main} is fault currents from the main grid, i_{micro} is fault currents from the microgrid; (c) Instantaneous active power of the converter; (d) DC voltage of the converter; (e) the converter's output currents.

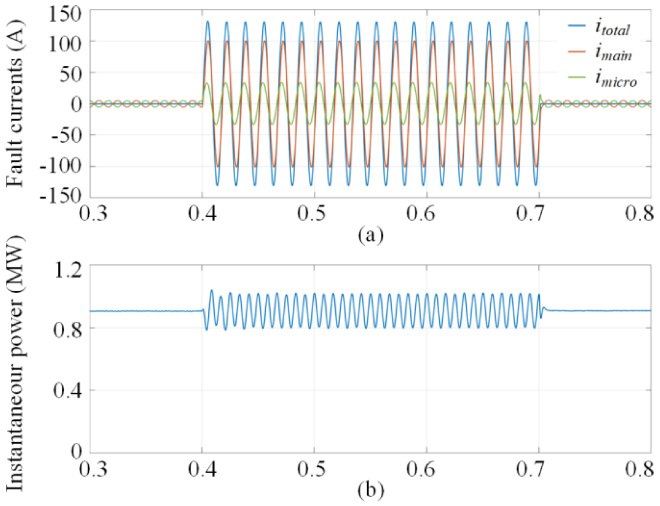

Fig. 5 Simulation results for single-phase-to-ground faults without AFM. (a) fault currents at fault location. (b) Instantaneous active power.

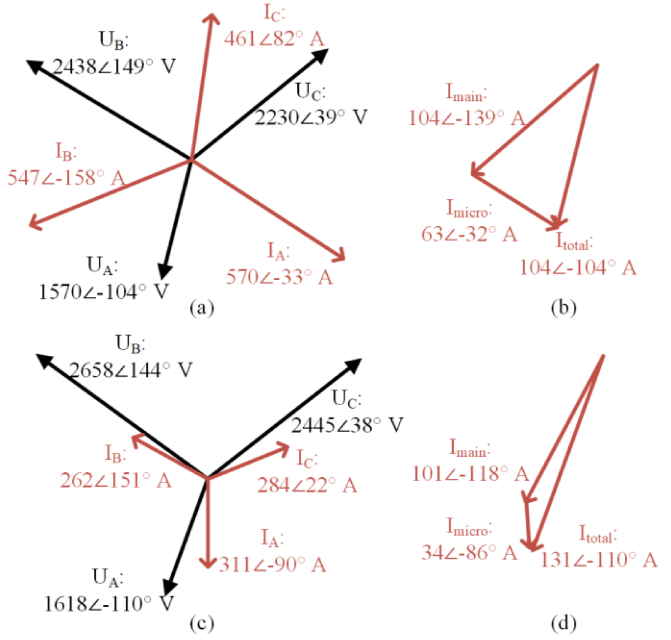

Fig. 6 Vector diagrams for single-phase-to-ground faults. (a) the converter's output voltages and currents and (b) fault currents at fault location with AFM; (c) the converter's output voltages and currents and (d) fault currents at fault location without AFM.

point c with coordinates (0%, 7.31%) and point c' with coordinates (10.0%, 44.27%) are chosen as simulation points. This means in single-phase-to-ground fault, the fault current contribution and the power ripples are controlled to be 0% and 7.31%, respectively. In double-phase-to-ground fault, the fault current contribution and the power ripples are controlled to be 10.0% and 44.3%, respectively.

C. *Single-phase-to-ground Fault*

For the single-phase-to-ground fault, the fault happens at 0.4s and is cleared at 0.7s. Fig. 4 shows the simulation results. As shown in Fig. 4 (b), at fault locations, three currents are measured. I_{main} is the fault currents from the main grid. I_{micro} is the fault currents from the microgrid. I_{total} is the total fault current to the ground and is also the algebraical sum of I_{main}

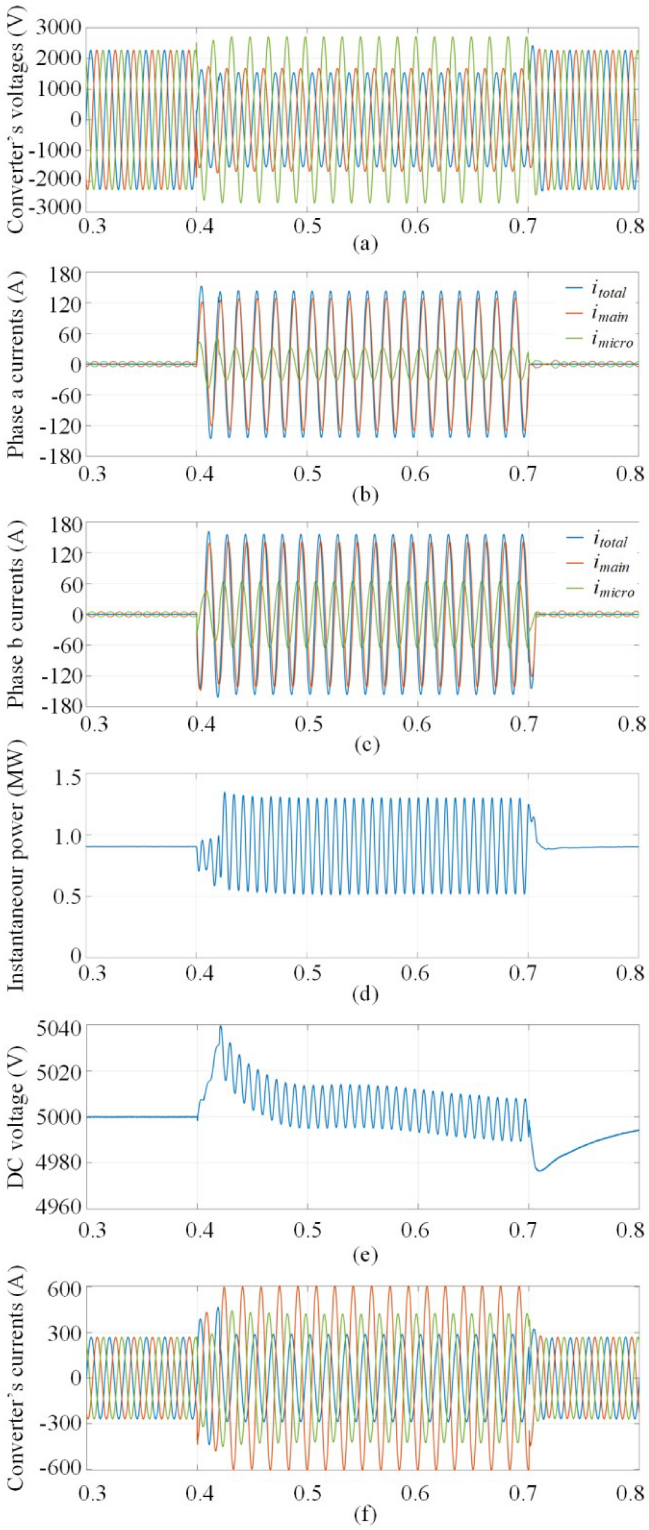

Fig. 7 Simulation results for double-phase-to-ground faults with AFM. (a) the converter's output voltages; (b) phase a and (c) phase b fault currents at fault location. i_{total} is the total fault currents to the ground, i_{main} is fault currents from the main grid, i_{micro} is fault currents from the microgrid; (c) Instantaneous active power of the converter; (d) DC voltage of the converter; (e) the converter's output currents.

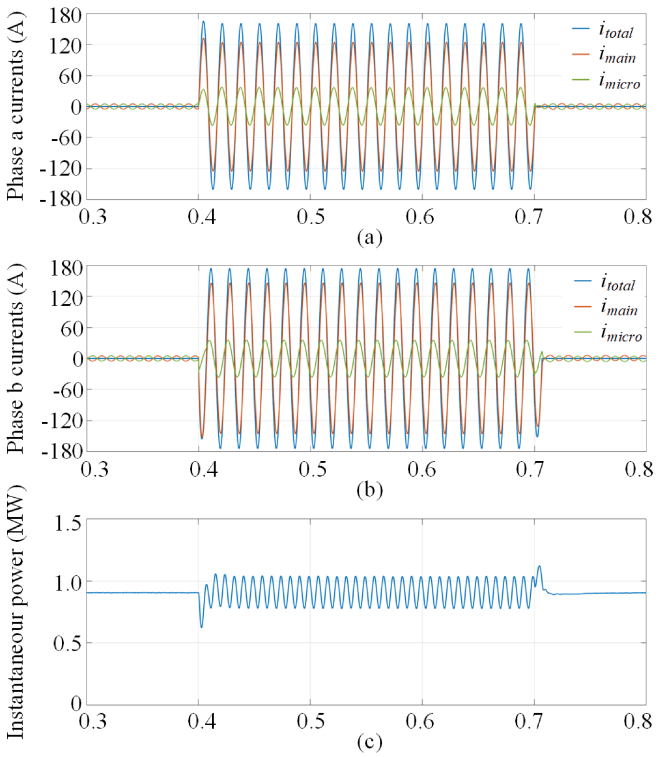

Fig. 8 Simulation results for double-phase-to-ground faults without AFM. (a) phase a and (b) phase b fault currents at the fault location; (c) Instantaneous active power.

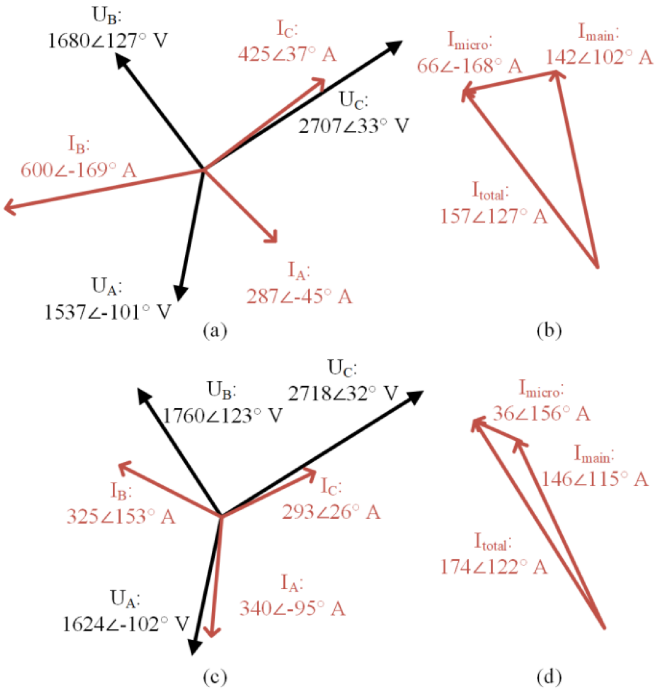

Fig. 9 Vector diagrams for two-phase-to-ground faults. (a) the converter's output voltages and currents and (b) phase b fault currents at fault location with AFM; (c) the converter's output voltages and currents and (d) phase b fault currents at fault location without AFM.

and I_{micro}. During faults, the amplitude of I_{total} is exactly the amplitude of I_{main}, which means the fault current contribution is 0%. Fig. 4 (c) shows instantaneous active power delivered

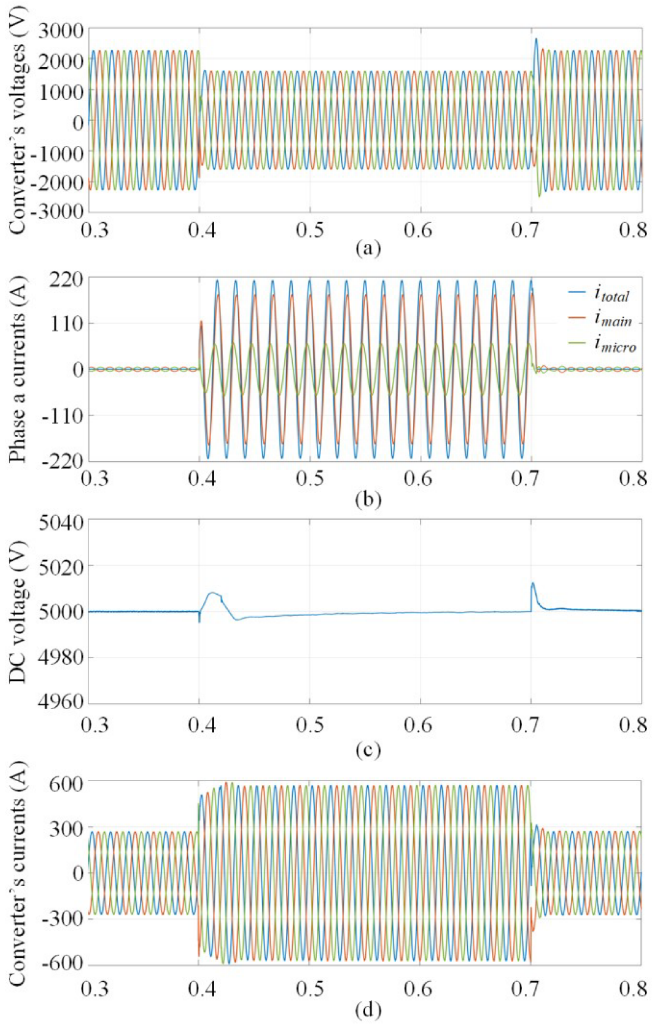

Fig. 10 Simulation results for three-phase-to-ground faults with AFM. (a) the converter's output voltages; (b) phase c fault currents at fault location. i_{total} is the total fault currents to the ground, i_{main} is fault currents from the main grid, i_{micro} is fault currents from the microgrid; (c) DC voltage of the converter; (d) the converter's output currents.

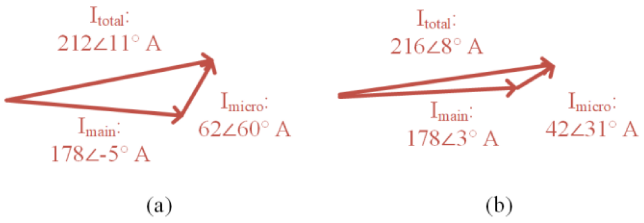

Fig. 11 Vector diagrams for three-phase-to-ground faults. Phase c fault currents at fault location (a) with AFM and (b) without AFM.

from GCC to the main grid. The double-line-frequency power ripple is 0.064 MW, which is 7.03% of the average delivered power. The simulation results match the operation point c with coordinates (0%, 7.31%) in Fig. 3. For comparison, Fig. 5 shows the simulation results for single-phase-to-ground faults without AFM. The amplitudes of I_{total} and I_{main} are 104 A and 130 A, respectively. This means that the connection of the microgrid

TABEL I COMPARISION BETWEEN AFM AND CONVENTIONAL RIDE-THROUGH METHOD

Fault type	AFM		Conventional ride-through method	
	Fault current contribution	Power ripples	Fault current contribution	Power ripples
Single-phase-to-ground	0.0%	7.03%	25.0%	9.01%
Double-phase-to-ground	10%	43.30%	26.73%	13.19%
Three-phase-to-ground	19.10%	0.0%	21.35%	0.0%

has contributed to increasing the amplitude of the total fault current by 26 A, a 25.0% contribution. The power ripple in Fig. 5 (b) is 0.082 MW, 9.01% of the average power.

Fig. 6 shows vector diagrams of GCC's output voltages and currents as well as fault currents at fault location. With the comparison between Fig. 6 (b) and Fig. 6 (d), it can be inferred that AFM controls the total fault current's amplitude by managing the phase angle of microgrid' currents.

D. Double-phase-to-ground Fault

The simulation results for double-phase-to-ground faults with AFM and without AFM are shown in Fig. 7 and Fig. 8, respectively. Phase a and phase b are fault phases and have sags of 30% at fault locations. The current contributions in Fig. 7 (b) and Fig. 7 (c) are 10%, and the power ripple in Fig. 7 (d) is 43.30%. The simulation results match the operation point c' with coordinates (10.0%, 44.27%) given in Fig. 3. Without AFM, the current contributions in phase a and phase b are 28.80% (125 A to 161 A) and 24.66% (146 A to 174A), respectively. The power ripple in Fig. 8 (c) is 13.19%. According to Pareto frontier in Fig. 3 (b), AFM can control the average current contribution and the power ripple to be (21.03%, 13.19%) and (26.73%, 1.85%), better than (26.73%, 13.19%) achieved without AFM. Vector diagrams for fault currents in Fig. 10 (b) and Fig. 10 (d) show AFM controls the total fault current's amplitude by managing the phase angle of microgrid' currents.

E. Three-phase-to-ground Fault

During three-phase-to-ground faults, power ripples in GCC's instantaneous active power is zero. Thus, AFM aims to minimize current contributions, as given in (1). Simulation results with AFM are shown in Fig. 10. The current contribution is 19.10% (from 178 A to 212 A). This is slightly better than results without AFM, in which the current contribution is 21.35%, as shown in Fig. 11.

F. Discussions about the simulation results

The comparison between AFM and the conventional ride through method is shown in Table I. In single-phase-to-ground faults and three-phase-to-ground faults, both fault current contributions and power ripples with AFM are better than the ones obtained by using the conventional ride through method. In double-phase-to-ground faults, the fault current contribution is better while the power ripples are worse. Yet, according to Pareto frontier in Fig. 3, other operation points can be chosen so that both fault current contribution and power ripples would be better with smaller magnitude of improvement. Similar conclusions can be achieved for different fault levels. AFM has used optimization method to identify the best trade-offs between fault current contribution and power ripples. Therefore, AFM can always get better or at least identical results compared with the results obtained with the conventional ride through method.

IV. CONCLUSION

This paper designs an active fault management (AFM) strategy to manage microgrids during balanced and unbalanced faults. The AFM adopts optimization method to identify optimal operation points and feedback control to ensure accuracy. Simulation results for different faults prove AFM's superiority in comparison to the conventional ride through method. In the future, AFM will be applied to networked microgrids. Also, reachability-analysis based AFM would be studied. AFM is used to control the interface converter between microgrids and the main grid. Therefore, AFM can also be used on other systems with converters, such as wind turbines and photovoltaic systems. Furthermore, the concept of combining optimization and feedback control can also be applied to other fields, such as robotics and manufacturing.

REFERENCE

[1] M. Khederzadeh and A. Beiranvand, "Identification and prevention of cascading failures in autonomous microgrid," *IEEE Syst. J.,* vol. 12, pp. 308-315, 2018.

[2] "IEEE Standard for interconnection and interoperability of distributed energy resources with associated electric power systems interfaces," *IEEE Std 1547-2018 (Revision of IEEE Std 1547-2003) - Redline,* pp. 1-227, 2018.

[3] "Distributed energy resources: connection, modeling, and reliability considerations," North American Electric Reliablility Corportation (NERC), 2017.

[4] P. Zhang and B. Wang, "Enabling reliable networked microgrids for distribution grid resiliency," NSF Award #1611095 University of Connecticut, 2016.

[5] L. Chen, H. Chen, J. Yang, L. Zhu, Y. Tang, L. H. Koh, *et al.*, "Comparison of superconducting fault current limiter and dynamic voltage restorer for LVRT improvement of high penetration microgrid," *IEEE Trans. Appl. Supercond.,* vol. 27, pp. 1-7, 2017.

[6] I. Syed and V. Khadkikar, "A dynamic voltage restorer (DVR) based interface scheme for microgrids," in *IECON 2014 - 40th Annual Conference of the IEEE Industrial Electronics Society*, 2014, pp. 5143-5149.

[7] N. Rajaei, M. H. Ahmed, M. M. A. Salama, and R. K. Varma, "Fault current management using inverter-based distributed generators in smart grids," *IEEE Trans. Smart Grid,* vol. 5, pp. 2183-2193, 2014.

[8] R. Kabiri, D. G. Holmes, and B. P. McGrath, "Control of active and reactive power ripple to mitigate unbalanced rrid voltages," *IEEE Trans. Ind. Appl.,* vol. 52, pp. 1660-1668, 2016.

[9] "Microgrids for data center," Pareto Energy, 2011.

[10] T. Hong and F. d. León, "Controlling Non-Synchronous Microgrids for Load Balancing of Radial Distribution Systems," *IEEE Trans. Smart Grid,* vol. 8, pp. 2608-2616, 2017.

[11] M. Di Somma, B. Yan, N. Bianco, G. Graditi, P. B. Luh, L. Mongibello, *et al.*, "Operation optimization of a distributed energy system considering energy costs and exergy efficiency," *Energy Convers. Manag.,* vol. 103, pp. 739-751, 2015/10/01/ 2015.